Published in final edited form as:

Curr Biol. 2017 July 24; 27(14): 2154–2162.e3. doi:10.1016/j.cub.2017.06.017.

Left habenular activity attenuates fear responses in larval zebrafish

Erik R. Duboué[1], **Elim Hong**[1,*], **Kiara C. Eldred**[2], and **Marnie E. Halpern**[1,2]

[1]Department of Embryology, Carnegie Institution for Science, 3520 San Martin Drive, Baltimore MD 21218

[2]Department of Biology, Johns Hopkins University, 3400 North Charles Street, Baltimore, MD 21218

Summary

Fear responses are defensive states that ensure survival of an organism in the presence of a threat. Perception of an aversive cue causes changes in behavior and physiology, such as freezing and elevated cortisol, followed by a return to the baseline state when the threat is evaded [1]. Neural systems that elicit fear behaviors include the amygdala, hippocampus and medial prefrontal cortex. However, aside from a few examples, little is known about brain regions that promote recovery from an aversive event [2]. Previous studies had implicated the dorsal habenular nuclei in regulating fear responses and boldness in zebrafish [3–7]. We now show that perturbation of the inherent left-right (L-R) asymmetry of the dorsal habenulo-interpeduncular (dHb-IPN) pathway at larval stages expedites the return of locomotor activity following an unexpected negative stimulus, electric shock. Severing habenular efferents to the IPN, or only those from the left dHb, prolongs the freezing behavior that follows shock. Individuals with symmetric, right isomerized dHb also exhibit increased freezing. In contrast, larvae that have symmetric, left-isomerized dHb, or in which just the left dHb-IPN projection is optogenetically activated, rapidly resume swimming post shock. In vivo calcium imaging reveals a neuronal subset, predominantly in the left dHb, whose activation is correlated with resumption of swimming. The results demonstrate functional specialization of the left dHb-IPN pathway in attenuating the response to fear.

Keywords

brain asymmetry; cortisol; anxiety; electric shock; calcium imaging

Corresponding Author (Lead Contact): Marnie E. Halpern, Department of Embryology Carnegie Institution for Science, 3520 San Martin, Drive, Baltimore MD 21218, tel.: 410-246-3018, halpern@ciwemb.edu.

*Current address: Laboratoire Neurosciences Paris Seine, INSERM UMRS 1130, UMR 8246 Université Pierre et Marie Curie 75252 Paris, France

Author Contributions

E.R.D., E.H. and M.E.H. designed the experiments. E.R.D., E.H. and K.C.E. conducted experiments and analyzed data. E.R.D. and M.E.H. wrote the manuscript with input from all authors.

Results

Larval zebrafish display a characteristic fear response post-shock

Spontaneous swimming in 7–8 day old (d) zebrafish larvae consists of alternating periods of short 'scoot'-like and fast 'burst'-like movements [8, 9]. Electric field stimulation (EFS; Figure S1A) induces three clearly distinguishable phases: (i) immediate hyperactivity [10], followed by (ii) a short period of inactivity and, finally, (iii) resumption of swimming (Movie S1). To establish the optimal stimulation intensity, larval responses to shock were measured across voltage intensities ranging from 0–100 V. Decreased locomotor activity post-shock, measured by the change in total distance traveled, as well as increased levels of the stress hormone, cortisol, were proportional to the intensity of the shock (Figure S1B, C). At 35 V (current density of 0.8 mA/cm^2), larvae reduce their locomotion by 50% during the first minute post-shock relative to activity determined 1 min prior (Figure 1B, S1D,E). By 4 min post-shock, locomotor activity is restored to pre-shock levels (Figure S1F).

We developed a metric for larval zebrafish (see Experimental Procedures) to measure the extent of freezing, which is a fear induced behavior defined by the absence of movement for an extended period of time [11]. Freezing was determined to correspond to periods of larval inactivity that exceeded 1.99 sec (Figure S1G), and is significantly increased post-shock (Figure S1H). The results confirm that mild shock elicits robust behavioral and physiological changes associated with fear in larval zebrafish.

Preferential role for left dHb-IPN pathway in mitigating fear

We tested the contribution of the dHb-IPN pathway in the larval fear response by severing habenular axon bundles in the fasciculus retroflexus (FR) using a multiphoton laser. Experiments were performed with transgenic larvae in which dHb neurons and their efferent axons are labeled with membrane-tagged green fluorescent protein (Figure 1A–D and Figure S2A, B). Locomotor activity post-shock was significantly decreased after severing of the bilateral FR or only the left bundle (Figure 1B′-C′, E and Figure S2C), and the duration of freezing was significantly increased (Figure 1F and Figure S2D). By contrast, larvae with the right FR severed showed locomotor activity comparable to controls (Figure 1D′, E, F). An intact left dHb-IPN pathway is, therefore, required for rapid resumption of swimming following electric shock.

To determine whether activation of the left dHb-IPN pathway is sufficient to reduce freezing duration post-shock, even at a higher voltage intensity (45 volts EFS), we unilaterally severed the FR in transgenic larvae expressing channelrhodopsin (ChR2) exclusively in the dHb (Figure 2A). We first determined that blue light exposure had no effect on spontaneous locomotor activity and that swimming behavior was indistinguishable between larvae that express ChR2 in the dHb and those that do not (Figure S3A–B and data not shown). However, when exposed to blue light (488 nm) immediately post-shock, larvae with both FR intact show significantly higher locomotor activity compared to controls that lack ChR2 expression or are not illuminated (Figure 2A–D). Upon optogenetic activation, individuals with only the left dHb-IPN pathway intact also exhibit increased locomotion (Figure 2B,E) and reduced freezing post-shock (Figure 2F) compared to those with just the right dHb-IPN

pathway activated (Figure 2A,B and E,F). Thus, left dHb function is not only required, but is also sufficient to signal resumption of swimming following a fearful cue.

Left-right identity of dHb influences fear responses

Directional asymmetry of the dHb can be altered in predictable ways in zebrafish. Ablation of the parapineal, an accessory organ to the pineal, results in right isomerization of the dHb, in which both nuclei develop symmetrically with right identity [12, 13]. Conversely, loss of canonical Wnt signaling in homozygous *tcf7l2* mutants causes left isomerization of the dHb [14]. Larvae with right isomerized dHb exhibit a significant reduction in locomotor activity post-shock (Figure 3A,B), increased duration of freezing (Figure 3C), and higher cortisol levels (Figure 3D), relative to controls with normal situs (*situs solitus*). By contrast, larvae with left isomerized dHb respond similarly to their wild-type siblings (Figure 3A–D). These manipulations, therefore, provide further evidence that dHb neurons with left identity have a preferential role in mitigating the response to fear.

Asymmetric activation of dHb neurons correlates with resumption of locomotion

To assess more directly neuronal activation of the dHb and how it relates to changes in locomotor behavior post-shock, we performed *in vivo* calcium imaging of the dHb in head affixed wild-type larvae. By measuring the angular velocity of their tails (Figure S3C), we found that these individuals also exhibit hyperactivity during shock, followed by a period of inactivity (35.61 ±9.8 sec, n=10, Figure S3D). Moreover, when exposed to blue light immediately post-shock, head affixed larvae that express ChR2 in the dHb resume tail movements significantly faster than siblings lacking the ChR2 transgene (14.5 ±1.6 and 34.3 ±4.5, respectively Figure S3D′). In the absence of EFS, ChR2-mediated activation of the dHb, by itself, did not alter spontaneous tail movements (Figure S3E,F). Thus, as with freely swimming larvae, optogenetic activation of the dHb of head affixed larvae expedites recovery post-shock.

Calcium transients were measured during the shock assay as the mean change in fluorescence intensity (ΔF/F) of GCaMP7a over time. Robust tail movements induced by electric shock in head affixed larvae cause motion artifacts in the scan field of the confocal microscope. We therefore paralyzed larvae by pre-exposing them to α-bungarotoxin prior to imaging, according to published methods [15–17]. Control experiments with rhodamine-conjugated α-bungarotoxin confirmed that the toxin labeled larval neuromuscular junctions, but did not penetrate the brain (Figure S4A).

Activation of individual dHb neurons (n=4195) from 38 wild-type zebrafish larvae was calculated from the area under the curve before and after shock, and the fold-change in GCaMP7a fluorescence fitted to a probability distribution function (refer to Experimental Procedures). Neurons were designated as responsive if the fold change post-shock exceeded 1 standard deviation of the mean (Figure S4A,B). It was noted that, as a group, responsive neurons showed less spontaneous activity than other dHb neurons (0.17 ±0.01 vs. 0.32 ±0.01 ΔF/F). Low spontaneous activity may, therefore, be a distinguishing feature of a neuronal population that responds to shock. Following shock, the majority of responsive neurons showed delayed activation with a 2.02 ±0.6 fold increase beginning at 17.5 ±5.01 sec (Figure

4A–C, left panel, Figure S4D,E and Movie S2). Only a small subset of dHb neurons (3.1%) responded within 1 sec post shock (Figure S4D,E). Approximately 20.2% ±2.0 of dHb neurons were responsive and these were asymmetrically distributed, with greater than 70% located in the left dHb (Figure 4D,E).

Perturbation of directional asymmetry of the dHb further corroborates that neurons with left identity are predominantly activated post-shock. In larvae with right isomerized dHb, few neurons (2.4% ±0.6) showed changes in GCaMP7a signaling after EFS (Figure 4D). A far greater percentage (30.0% ±4.1) were responsive In larvae with left isomerized dHb and these neurons were distributed equally in both dHb (Figure 4D,E). The described manipulations of the dHb-IPN pathway in larval zebrafish support a role for asymmetric activation of the dHb in promoting the return to locomotor behavior following a fearful event.

Discussion

Preferential activation of left dHb neurons, or disruption of their function by cellular and genetic manipulations, demonstrate that the left dHb-IPN pathway is required for attenuating innate fear in larval zebrafish. Left-right differences in neuronal subtypes, afferent input and/or connectivity with the IPN could underlie the observed functional lateralization of the dHb.

All dHb neurons are glutamatergic in zebrafish larvae, but the right nucleus contains larger populations that are also cholinergic and somatostatinergic [18, 19]. The predominance of neurons in the left dHb that are activated post-shock suggests that they are not cholinergic but rather are solely glutamatergic or express other asymmetrically distributed co-transmitters such as Substance P (SP) [19]. In support of a role for this peptide, genetic ablation of afferents to SPergic neurons of the mouse medial Hb leads to prolonged freezing following an unexpected footshock, whereas disruption of septal inputs to cholinergic neurons has no effect [20].

With respect to afferent connections, the zebrafish dHb receives input from the olfactory bulb, pallium, eminentia thalami (EmT), and the entopeduncular nucleus [21–24]. Notably, axons from a bilaterally distributed subset of olfactory mitral cells terminate in a discrete region of only the right dHb [25]. The left dHb was recently shown to receive visual input from a specific type of retinal ganglion cell via EmT afferent connections [26]. In agreement with these differences in connectivity, the left and right dHb differentially respond to light and odor cues [26–28]. Since only 20% of left dHb neurons are light-responsive [27], most likely they comprise a distinct set than those that attenuate fear.

The dHb also show differences in their efferent projections to the IPN: Distinct neuronal populations in the left dHb innervate the dorsal and ventral IPN, whereas the right dHb largely innervates the ventral IPN and to a far lesser extent the dorsal region [3, 29]. This has important functional consequences, as dorsal IPN neurons project to the griseum centrale [3] (analogous to the periaqueductal gray [30]), an area involved in coping with stressful events [31, 32]. We suspect that, following shock, an increase in neuronal activity, predominantly in

the left dHb, gradually leads to stimulation of the dorsal IPN. Accumulating dHb input to the dorsal IPN would, in turn, modulate neurons in the griseum centrale, ultimately mitigating fear and promoting recovery.

The link between asymmetric neural function and fear/anxiety responses may be a general feature of the vertebrate brain. One contested [33] theory, the valence hypothesis, proposes that positive and negative stimuli are differentially processed by the left and right sides of the brain [34]. Indeed, functional MRI reveals activation of the left prefrontal cortex when humans view images perceived as pleasant, and of the right prefrontal cortex for images that elicit negative emotional responses [33, 35, 36]. In rats, a food reward increases neural activity and norepinephrine (NE) release in the left basolateral amygdala (BLA), whereas foot shock causes increased activity and NE release in the right BLA [37, 38]. After fear conditioning in rats, the level of protein kinase C expression is also higher in the right amygdala than the left and is correlated with freezing duration [39]. Interestingly, a recent report describing fighting behavior in adult zebrafish suggests that winning is associated with activation of the left dHb and losing with the right [4]. Whether boldness is conferred on adult zebrafish through the same neurons that we show promote recovery from fear in larvae is an intriguing issue to resolve. Accumulating evidence in studies from fish to humans indicates that left-right differences in neural responses are highly correlated with the emotional content of the stimulus.

STAR ★ METHODS

CONTACT FOR REAGENT AND RESOURCE SHARING

Further information and requests for resources and reagents should be directed to and will be fulfilled by the Lead Contact Marnie E. Halpern (Halpern@ciwemb.edu)

EXPERIMENTAL MODEL AND SUBJECT DETAILS

Wild-type AB [40] and *tcf7l2*^{zf55} mutant strains [41] and the transgenic lines *Tg(foxd3:gfp)*^{fkg17}, *TgBAC(gng8:nfsB-EGFP-CAAX)*^{c375}, *TgBAC(gng8:gal4ff)*^{c426}, *Tg(UAS:ChR2(H134R)-mCherry)*^{s1985t} and *Tg(UAS:GCaMP7a)* [19, 42–45] were used. Approximately 10 adults per liter were maintained at 27°C on a 14:10 light:dark cycle in a recirculating system with dechlorinated, filtered and UV treated system water. Experiments were carried out between 11 a.m. to 6 p.m., and according to a protocol (#122) approved by the Institutional Animal Care and Use Committee of the Carnegie Department of Embryology.

METHODS DETAILS

Manipulation of Hb-IPN pathway—For severing of the fasciculus retroflexus (FR), 3 day old (d) *TgBAC(gng8:nfsB-EGFP-CAAX)*^{c375} larvae were anesthetized in 0.02% tricaine (Sigma) and mounted dorsal side up in 1.5% low-melt agarose (Seaplaque, Lonza). The FR was located under a Leica SP5 confocal microscope and a MaiTai multiphoton laser (Spectra Physics) focused over the axon tract. The laser was activated at 885 nm for 2 seconds, which applied a 100 mW pulse over an area of 9.5–12 um^2. The laser power was measured using a Newport power meter (model 1918-C). This procedure was repeated 2 d

later to ensure complete transection of newly emerged Hb efferents. Controls were not exposed to the laser or received lesions in regions medial or lateral to the FR. Confocal Z-stacks were obtained at 3 d before and after severing the FR, and 5 d later following behavioral testing. Maximum projections of confocal images were generated in FIJI.

Larvae with right isomerized habenulae were obtained by laser-mediated ablation of the parapineal at 3 d [5, 13]. *Tg(foxd3:gfp)*^{fkg17} larvae were anesthetized in 0.02% tricaine and mounted dorsal side up in 1.5% low-melt agarose. GFP labeled parapineal cells were visualized under the confocal microscope and destroyed by laser scanning at 30–40% power. For controls, the laser was focused to the right of the pineal, contralateral to the parapineal.

Behavioral assays—All behavioral experiments were performed blind as to the dHb-IPN phenotype of the larva being assayed. Larvae from single clutches were tested and, where relevant, their siblings used as controls (n=>3 trials).

Shock assay on freely swimming larvae: Behavioral tests were conducted on 7–8 d larvae, which were acclimated in a temperature controlled room. A 6 cm^3 chamber was constructed out of clear acrylic (0.5 cm thick). Two pairs of stainless steel mesh electrodes (6 cm^2) were mounted to the walls and separated by a rubber insulator. Electrodes were connected to a Grass SD9 electrical stimulator (Natus Neurology, RI). A cell strainer (40 mm, BD Falcon) was placed on top of a 0.5 cm platform and filled with fresh system water. The chamber was positioned above an infrared illumination source (880 nm, ViewPoint Life Sciences, Lyon, France) and below a high frame rate charged couple device (CCD) camera (Point Grey Research) connected to a computer (Dell). Larvae were tracked in real-time at 60 frames per sec with ZebraLab software (ViewPoint Life Sciences, Lyon, France). Locomotor activity was recorded for 1 min pre-shock, during electrical field stimulation (30V, 5 pulses, 1 pulse per sec, 200 msec duration), and for 1 min post-shock (Movie S1). For optogenetic activation, a blue LED (488 nm, Thor Labs) was mounted over the chamber and larvae were immediately exposed to blue light for 5 sec post-shock. The intensity of blue light was calculated to be 1 mW/cm^2, and was measured using and light meter (Extech, model 401025). Locomotor activity was recorded during a 1 min pre-shock, during electrical field stimulation (45V, 5 pulses, 1 pulse per sec, 200 msec duration) and for 1 min post-shock.

For the analysis of locomotor activity, the x and y coordinates of larval position in each frame were exported from ZebraLab, and activity was quantified using a custom written script in R according to the distance equation:

$$D=\sqrt{(x_{i+1}-x_i)^2+(y_{i+1}-y_i)^2}$$

where i corresponds to a single frame. Total distance traveled was calculated by summing the distance per frame over the entire pre- or post-shock phases. To counter the effect of occasional erratic movements, the total distance traveled and freezing duration were compared between the full 1 min pre- and post-shock intervals. Activity plots were generated by displaying total distance traveled within 1 sec bins.

To develop a metric for freezing, 6028 periods of immobility were measured in 44 wild-type larvae. The log2 of immobility periods was used to transform the data to a Gaussian Distribution and a probability distribution function was fit using the '*fitnorm'* function of the *'fitditrplus'* software package in R [46]. Freezing was defined as a period of immobility that exceeded the 5% area (i.e., p=0.05) on the right side of the curve, computed using the *'pnorm'* function.

To assess dHb left-right phenotype after behavioral testing, larvae derived from *tcf7l2*^{zf55} heterozygous matings or from parapineal ablation experiments were transferred to 0.5 ml tubes, fixed in 4% paraformaldehyde, and processed for RNA in situ hybridization, as described [19].

Shock assay on head affixed larvae: Individual larvae were embedded dorsal side up in a drop of 1.5% low melt agarose in the center of a 60 mm petri dish. Agarose was gently removed from the tail and pectoral fins using a tungsten needle, and the head affixed larvae allowed to recover for 20 min. A pair of stainless steel electrodes (4 × 1 cm) were fixed to the inner walls of a polyvinyl chloride (PVC) ring (outer diameter = 50 mm; inner diameter = 40 mm; thickness = 10 cm) with dental wax. The electrodes were connected to the SD9 stimulator and placed inside the petri dish parallel to the length of the larva. This set-up generated a current density that was measured to be equivalent to that use in freely swimming larvae. Larvae were recorded for 5 min, shocked once (20V, 200 msec), and recorded for 1 additional min. For optogenetic activation, a blue LED (488 nm, Thor Labs) was mounted over the chamber and larvae were immediately exposed to blue light for 5 sec post-shock (1 mW/cm^2).

The angular velocity of tail movements was analyzed offline using custom written MATLAB (version R2015a, Mathworks) scripts. Briefly, the larval form was converted to a binary image using the 'im2bw' function and reduced to a single medial line using the *'bwmorph'* function with the *'skel'* attribute specified [47]. A point was drawn manually at the head of the larva using the *'getpts'* function, and the software calculated the end of the tail. Using the (x_{head}, y_{head}) and (x_{tail}, y_{tail}) points, the angle of the tail was calculated for all frames in the movie according to the formula:

$$\theta = rad2\deg\left(atan\left(\frac{x_{tail} - x_{head}}{y_{tail} - y_{head}}\right)\right)$$

Cortisol measurements—Whole body cortisol levels were measured using a modified protocol [48, 49]. Pools of 7–8 d larvae were maintained overnight in a cell strainer (40 mm, BD Falcon) inside a petri dish filled with system water. The strainer was transferred to the behavior chamber and larvae were shocked five times (30V, 1 pulse per sec, 200 msec) and returned to a petri dish. The control group received no stimulation. After 10 min recovery, larvae were euthanized in tricaine and transferred to a glass vial.

To extract cortisol, larvae were ground in 1 ml ice-cold 1X phosphate buffered saline (PBS) using a glass mortar and pestle. A small aliquot of the homogenate was transferred to a 1.5 ml tube for protein measurements. Total protein levels were calculated using a Quick Start

Bradford assay (BioRad) with bovine serum albumin as a standard. Diethyl ether (2 ml, Sigma) was added to the homegenate using a glass pipette, the mixture vortexed for 1 min, and centrifuged at 5000 rpm at 4°C for 10 min. The top layer containing glucocorticoids was transferred to a glass borosilicate tube (VWR) and placed under a fume hood. The diethyl ether extraction was repeated twice. After evaporation, the residue was reconstituted in 1 ml 1X PBS and left at 4°C for 24 hours. Cortisol levels were assayed using an ELISA kit (Sallimetrics, State College, PA), and the final reaction analyzed using a SpectraMax M5 plate reader (Molecular Devices) set to 450 nm.

Calcium Imaging—Calcium imaging of the dHb was performed using *TgBAC(gng8:gal4ff)*^{c426}; *Tg(UAS:GCaMP7a)* larvae. All experiments were performed blind as to the phenotype of the larvae being assayed.

To minimize movement artifacts, larvae were paralyzed by a 1 min exposure to α-bungarotoxin (Life Technologies) or Rhodamine-conjugated α-bungarotoxin (Sigma; 1 mg/ml in system water) followed by washing in fresh system water, in accordance with methods routinely used for 7–8 d zebrafish larvae [15–17]. Paralyzed larvae were individually embedded dorsal side up in 1.5% low melt agarose in a Petri dish (60 mm). After the agarose solidified, system water was added and the PVC ring holding the electrodes was placed inside the dish. The dish was positioned under a 25X (NA=0.95) water immersion objective mounted on a Leica SP5 laser scanning confocal microscope. GCaMP7a was excited in the dHb using a 488 nm argon laser. Images were acquired in *xyt* acquisition mode at 512 × 200 pixel resolution at a rate of 5Hz. At least 1000 frames were collected to score the baseline spontaneous activity for individual neurons. Larvae were shocked once (20V, 200 msec pulse duration), and neuronal activity in the dHb recorded for an additional 1000 frames.

Mean fluorescence intensity was calculated for individual neurons in FIJI [50]. Briefly, a high-contrast image of the dHb was generated by averaging all frames using the '*Z Project*' function, and regions of interest (ROI) were manually drawn around each cell in the focal plane with the polygon tool and '*ROI Manager function*'. The set of ROIs were saved as a .zip file. Mean fluorescence intensity values per frame were calculated for each ROI using the '*Multi Measure*' function and the resulting data saved as an Excel file (Microsoft).

The high-contrast image of the dHb, the set of ROIs, and the values of mean fluorescence intensity were imported into MATLAB (version R2015a, Mathworks), where ΔF/F [51] was calculated according to the formula:

$$F \leftarrow \left(\frac{F_i - F_{min}}{F_{max} - F_{min}} \right)$$

where F_i is the mean fluorescence intensity in an ROI at a single time point, F_{max} and F_{min} indicate the maximum and minimum fluorescence for that neuron over the entire recording period. Total activity for each neuron before and after shock was calculated from the area under the curve, according to the trapezoid approximation with the MATLAB function *'trapz'*. The natural log fold change in fluorescence was fit to a normal distribution and the

mean and standard deviation determined. Neurons were deemed responsive if the change in fluorescence intensity post-shock was greater than 1 standard deviation of the mean [52, 53], and responsive neurons on average had a greater than 2-fold increase in neural activity [54]. The initial time point at which neuronal activity increased, for a given neuron, was determined using the MATLAB function '*findpeaks*'.

QUANTIFICATION AND STATISTICAL ANALYSIS

Statistical analyses were nonparametric and performed using GraphPad Prism 6 (GraphPad Software, Inc.). The Wilcoxon signed rank test was used for comparisons between related samples, the nonparametric Mann-Whitney U test for comparisons between two groups, and the Kruskal-Wallis one-way ANOVA for comparisons between more than two groups. When statistical significance between groups was obtained, the Dunn's post-test with correction for multiple comparisons was performed. Sample sizes were in accord with or exceeded those typically used in zebrafish behavior and calcium imaging studies [5, 6, 27, 28, 55, 56].

Supplementary Material

Refer to Web version on PubMed Central for supplementary material.

Acknowledgments

The authors are grateful to Akira Muto and Koichi Kawakami (National Institute of Genetics) for generously providing the *Tg(UAS:GCaMP7a)* line prior to publication. We thank Allen Strause and Kevin Smolenski for constructing behavioral apparatus, and Rejji Kuruvilla and Filippo del Bene for their helpful feedback. This work was supported by a grant from the National Institute of Child Health and Human Development 5R01HD042215 (M.E.H.).

References

1. Goldstein DS, McEwen B. Allostasis, homeostats, and the nature of stress. Stress. 2002; 5:55–58. [PubMed: 12171767]
2. Tovote P, Fadok JP, Luthi A. Neuronal circuits for fear and anxiety. Nat Rev Neurosci. 2015; 16:317–331. [PubMed: 25991441]
3. Agetsuma M, Aizawa H, Aoki T, Nakayama R, Takahoko M, Goto M, Sassa T, Amo R, Shiraki T, Kawakami K, et al. The habenula is crucial for experience-dependent modification of fear responses in zebrafish. Nat Neurosci. 2010; 13:1354–1356. [PubMed: 20935642]
4. Chou MY, Amo R, Kinoshita M, Cherng BW, Shimazaki H, Agetsuma M, Shiraki T, Aoki T, Takahoko M, Yamazaki M, et al. Social conflict resolution regulated by two dorsal habenular subregions in zebrafish. Science. 2016; 352:87–90. [PubMed: 27034372]
5. Facchin L, Burgess HA, Siddiqi M, Granato M, Halpern ME. Determining the function of zebrafish epithalamic asymmetry. Philos Trans R Soc Lond B Biol Sci. 2009; 364:1021–1032. [PubMed: 19064346]
6. Facchin L, Duboue ER, Halpern ME. Disruption of Epithalamic Left-Right Asymmetry Increases Anxiety in Zebrafish. J Neurosci. 2015; 35:15847–15859. [PubMed: 26631467]
7. Lee A, Mathuru AS, Teh C, Kibat C, Korzh V, Penney TB, Jesuthasan S. The habenula prevents helpless behavior in larval zebrafish. Curr Biol. 2010; 20:2211–2216. [PubMed: 21145744]
8. Budick SA, O'Malley DM. Locomotor repertoire of the larval zebrafish: swimming, turning and prey capture. The Journal of experimental biology. 2000; 203:2565–2579. [PubMed: 10934000]
9. Burgess HA, Granato M. Sensorimotor gating in larval zebrafish. J Neurosci. 2007; 27:4984–4994. [PubMed: 17475807]

10. Tabor KM, Bergeron SA, Horstick EJ, Jordan DC, Aho V, Porkka-Heiskanen T, Haspel G, Burgess HA. Direct activation of the Mauthner cell by electric field pulses drives ultrarapid escape responses. J Neurophysiol. 2014; 112:834–844. [PubMed: 24848468]
11. Fanselow MS. Factors governing one-trial contextual conditioning. Animal Learning & Behavior. 1990; 18:264–270.
12. Concha ML, Burdine RD, Russell C, Schier AF, Wilson SW. A nodal signaling pathway regulates the laterality of neuroanatomical asymmetries in the zebrafish forebrain. Neuron. 2000; 28:399–409. [PubMed: 11144351]
13. Gamse JT, Thisse C, Thisse B, Halpern ME. The parapineal mediates left-right asymmetry in the zebrafish diencephalon. Development. 2003; 130:1059–1068. [PubMed: 12571098]
14. Husken U, Stickney HL, Gestri G, Bianco IH, Faro A, Young RM, Roussigne M, Hawkins TA, Beretta CA, Brinkmann I, et al. Tcf7l2 is required for left-right asymmetric differentiation of habenular neurons. Curr Biol. 2014; 24:2217–2227. [PubMed: 25201686]
15. Baraban SC. Forebrain electrophysiological recording in larval zebrafish. J Vis Exp. 2013
16. Hong S, Lee P, Baraban SC, Lee LP. A Novel Long-term, Multi-Channel and Non-invasive Electrophysiology Platform for Zebrafish. Sci Rep. 2016; 6:28248. [PubMed: 27305978]
17. Severi KE, Portugues R, Marques JC, O'Malley DM, Orger MB, Engert F. Neural control and modulation of swimming speed in the larval zebrafish. Neuron. 2014; 83:692–707. [PubMed: 25066084]
18. deCarvalho TN, Subedi A, Rock J, Harfe BD, Thisse C, Thisse B, Halpern ME, Hong E. Neurotransmitter map of the asymmetric dorsal habenular nuclei of zebrafish. Genesis. 2014; 52:636–655. [PubMed: 24753112]
19. Hong E, Santhakumar K, Akitake CA, Ahn SJ, Thisse C, Thisse B, Wyart C, Mangin JM, Halpern ME. Cholinergic left-right asymmetry in the habenulo-interpeduncular pathway. Proc Natl Acad Sci U S A. 2013; 110:21171–21176. [PubMed: 24327734]
20. Yamaguchi T, Danjo T, Pastan I, Hikida T, Nakanishi S. Distinct roles of segregated transmission of the septo-habenular pathway in anxiety and fear. Neuron. 2013; 78:537–544. [PubMed: 23602500]
21. Amo R, Fredes F, Kinoshita M, Aoki R, Aizawa H, Agetsuma M, Aoki T, Shiraki T, Kakinuma H, Matsuda M, et al. The habenulo-raphe serotonergic circuit encodes an aversive expectation value essential for adaptive active avoidance of danger. Neuron. 2014; 84:1034–1048. [PubMed: 25467985]
22. Hendricks M, Jesuthasan S. Asymmetric innervation of the habenula in zebrafish. J Comp Neurol. 2007; 502:611–619. [PubMed: 17394162]
23. Mueller T, Guo S. The distribution of GAD67-mRNA in the adult zebrafish (teleost) forebrain reveals a prosomeric pattern and suggests previously unidentified homologies to tetrapods. J Comp Neurol. 2009; 516:553–568. [PubMed: 19673006]
24. Turner KJ, Hawkins TA, Yanez J, Anadon R, Wilson SW, Folgueira M. Afferent Connectivity of the Zebrafish Habenulae. Frontiers in neural circuits. 2016; 10:30. [PubMed: 27199671]
25. Miyasaka N, Morimoto K, Tsubokawa T, Higashijima S, Okamoto H, Yoshihara Y. From the olfactory bulb to higher brain centers: genetic visualization of secondary olfactory pathways in zebrafish. J Neurosci. 2009; 29:4756–4767. [PubMed: 19369545]
26. Zhang BB, Yao YY, Zhang HF, Kawakami K, Du JL. Left Habenula Mediates Light-Preference Behavior in Zebrafish via an Asymmetrical Visual Pathway. Neuron. 2017; 93:914–928 e914. [PubMed: 28190643]
27. Dreosti E, Vendrell Llopis N, Carl M, Yaksi E, Wilson SW. Left-right asymmetry is required for the habenulae to respond to both visual and olfactory stimuli. Curr Biol. 2014; 24:440–445. [PubMed: 24508167]
28. Jetti SK, Vendrell-Llopis N, Yaksi E. Spontaneous activity governs olfactory representations in spatially organized habenular microcircuits. Curr Biol. 2014; 24:434–439. [PubMed: 24508164]
29. Gamse JT, Kuan YS, Macurak M, Brosamle C, Thisse B, Thisse C, Halpern ME. Directional asymmetry of the zebrafish epithalamus guides dorsoventral innervation of the midbrain target. Development. 2005; 132:4869–4881. [PubMed: 16207761]

30. Okamoto H, Agetsuma M, Aizawa H. Genetic dissection of the zebrafish habenula, a possible switching board for selection of behavioral strategy to cope with fear and anxiety. Developmental neurobiology. 2012; 72:386–394. [PubMed: 21567982]
31. Bandler R, Keay KA. Columnar organization in the midbrain periaqueductal gray and the integration of emotional expression. Prog Brain Res. 1996; 107:285–300. [PubMed: 8782526]
32. Bandler R, Keay KA, Floyd N, Price J. Central circuits mediating patterned autonomic activity during active vs. passive emotional coping. Brain Res Bull. 2000; 53:95–104. [PubMed: 11033213]
33. Killgore WD, Yurgelun-Todd DA. The right-hemisphere and valence hypotheses: could they both be right (and sometimes left)? Soc Cogn Affect Neurosci. 2007; 2:240–250. [PubMed: 18985144]
34. Davidson, R. Affect, cognition and hemispheric specialization. In: Izard, C.Kagan, J., Zajonc, R., editors. Emotion, Cognition and Behavior. New York: Cambridge; 1984.
35. Beraha E, Eggers J, Hindi Attar C, Gutwinski S, Schlagenhauf F, Stoy M, Sterzer P, Kienast T, Heinz A, Bermpohl F. Hemispheric asymmetry for affective stimulus processing in healthy subjects–a fMRI study. PLoS One. 2012; 7:e46931. [PubMed: 23056533]
36. Canli T, Desmond JE, Zhao Z, Glover G, Gabrieli JD. Hemispheric asymmetry for emotional stimuli detected with fMRI. Neuroreport. 1998; 9:3233–3239. [PubMed: 9831457]
37. Young EJ, Williams CL. Valence dependent asymmetric release of norepinephrine in the basolateral amygdala. Behav Neurosci. 2010; 124:633–644. [PubMed: 20939663]
38. Young EJ, Williams CL. Differential activation of amygdala Arc expression by positive and negatively valenced emotional learning conditions. Front Behav Neurosci. 2013; 7:191. [PubMed: 24367308]
39. Orman R, Stewart M. Hemispheric differences in protein kinase C betaII levels in the rat amygdala: baseline asymmetry and lateralized changes associated with cue and context in a classical fear conditioning paradigm. Neuroscience. 2007; 144:797–807. [PubMed: 17118565]
40. Walker C. Haploid screens and gamma-ray mutagenesis. Methods in cell biology. 1999; 60:43–70. [PubMed: 9891330]
41. Muncan V, Faro A, Haramis AP, Hurlstone AF, Wienholds E, van Es J, Korving J, Begthel H, Zivkovic D, Clevers H. T-cell factor 4 (Tcf7l2) maintains proliferative compartments in zebrafish intestine. EMBO reports. 2007; 8:966–973. [PubMed: 17823612]
42. Arrenberg AB, Del Bene F, Baier H. Optical control of zebrafish behavior with halorhodopsin. Proc Natl Acad Sci U S A. 2009; 106:17968–17973. [PubMed: 19805086]
43. deCarvalho TN, Akitake CM, Thisse C, Thisse B, Halpern ME. Aversive cues fail to activate fos expression in the asymmetric olfactory-habenula pathway of zebrafish. Frontiers in neural circuits. 2013; 7:98. [PubMed: 23734103]
44. Gilmour DT, Maischein HM, Nusslein-Volhard C. Migration and function of a glial subtype in the vertebrate peripheral nervous system. Neuron. 2002; 34:577–588. [PubMed: 12062041]
45. Muto A, Ohkura M, Abe G, Nakai J, Kawakami K. Real-time visualization of neuronal activity during perception. Curr Biol. 2013; 23:307–311. [PubMed: 23375894]
46. Delignette-Muller M, Dutang C. fitdistrplus: An R Package for Fitting Distributions. Journal of Statistical Software. 2015; 64:1–34.
47. Huang KH, Ahrens MB, Dunn TW, Engert F. Spinal projection neurons control turning behaviors in zebrafish. Curr Biol. 2013; 23:1566–1573. [PubMed: 23910662]
48. Cachat J, Stewart A, Grossman L, Gaikwad S, Kadri F, Chung KM, Wu N, Wong K, Roy S, Suciu C, et al. Measuring behavioral and endocrine responses to novelty stress in adult zebrafish. Nature protocols. 2010; 5:1786–1799. [PubMed: 21030954]
49. Steenbergen, P., Metz, J., Flik, G., Richardson, M., Champagne, D. Methods to Quantify Basal and Stress-Induced Cortisol Response in Larval Zebrafish. In: Kalueff, AV., Stewart, AM., editors. Zebrafish Protocols for Neurobehavioral Research. Vol. 66. Humana Press; 2012. p. 121-141.
50. Schindelin J, Arganda-Carreras I, Frise E, Kaynig V, Longair M, Pietzsch T, Preibisch S, Rueden C, Saalfeld S, Schmid B, et al. Fiji: an open-source platform for biological-image analysis. Nature methods. 2012; 9:676–682. [PubMed: 22743772]

51. Vogelstein JT, Packer AM, Machado TA, Sippy T, Babadi B, Yuste R, Paninski L. Fast nonnegative deconvolution for spike train inference from population calcium imaging. J Neurophysiol. 2010; 104:3691–3704. [PubMed: 20554834]

52. Berdyyeva TK, Frady EP, Nassi JJ, Aluisio L, Cherkas Y, Otte S, Wyatt RM, Dugovic C, Ghosh KK, Schnitzer MJ, et al. Direct Imaging of Hippocampal Epileptiform Calcium Motifs Following Kainic Acid Administration in Freely Behaving Mice. Front Neurosci. 2016; 10:53. [PubMed: 26973444]

53. Briggs SW, Walker J, Asik K, Lombroso P, Naegele J, Aaron G. STEP regulation of seizure thresholds in the hippocampus. Epilepsia. 2011; 52:497–506. [PubMed: 21204826]

54. Krishnan S, Mathuru AS, Kibat C, Rahman M, Lupton CE, Stewart J, Claridge-Chang A, Yen SC, Jesuthasan S. The right dorsal habenula limits attraction to an odor in zebrafish. Curr Biol. 2014; 24:1167–1175. [PubMed: 24856207]

55. Dunn TW, Gebhardt C, Naumann EA, Riegler C, Ahrens MB, Engert F, Del Bene F. Neural Circuits Underlying Visually Evoked Escapes in Larval Zebrafish. Neuron. 2016; 89:613–628. [PubMed: 26804997]

56. Filosa A, Barker AJ, Dal Maschio M, Baier H. Feeding State Modulates Behavioral Choice and Processing of Prey Stimuli in the Zebrafish Tectum. Neuron. 2016; 90:596–608. [PubMed: 27146269]

Highlights

- An assay was devised to measure fear responses, such as freezing, in larval zebrafish
- Disrupting the left dHb-IPN pathway prolongs freezing behavior
- Freezing is reduced following optogenetic activation of the left dHb
- Neuronal activity largely in the left dHb correlates with resumption of locomotion

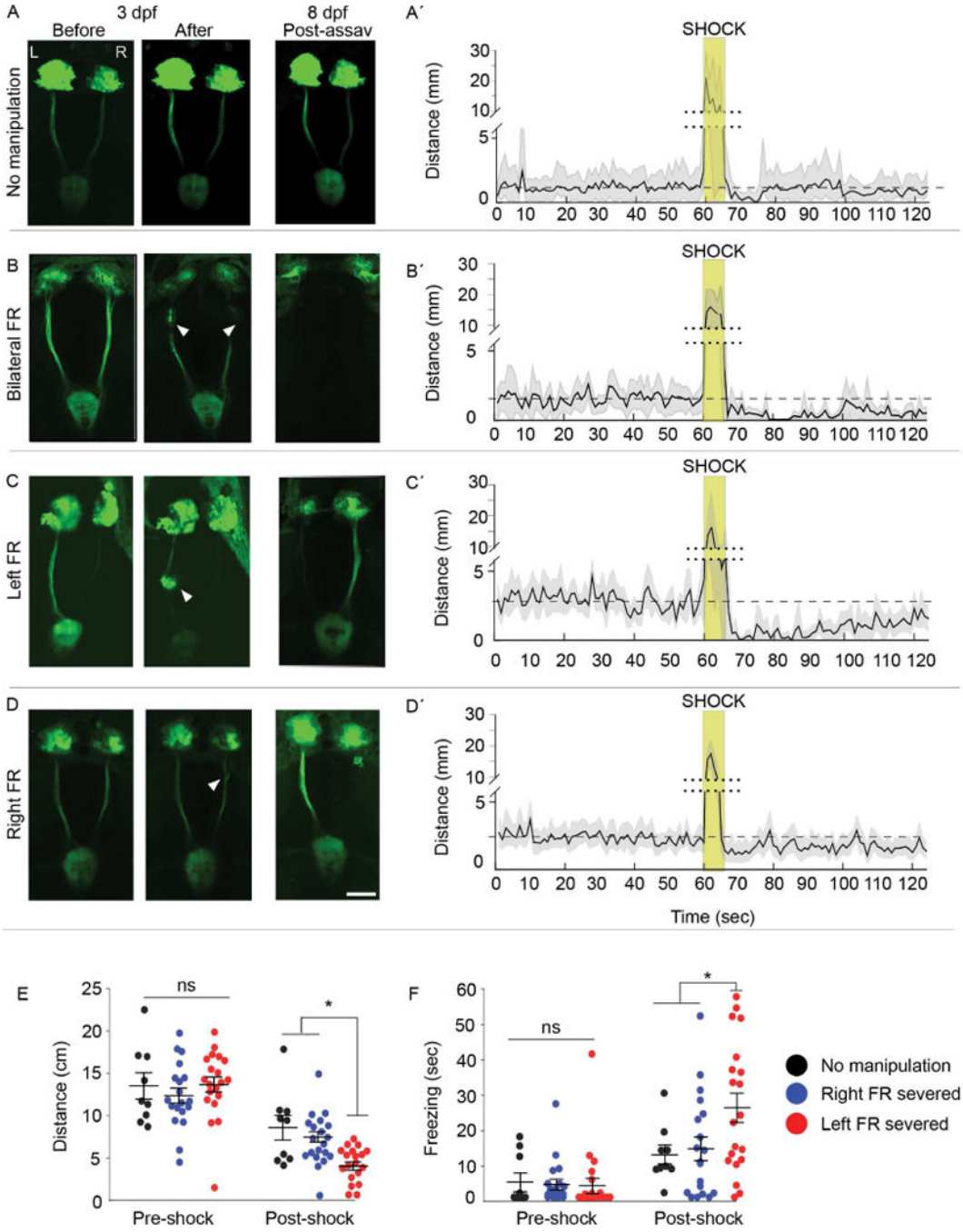

Fig. 1. Intact left dHb-IPN pathway required to mitigate fear behaviors

(A–D) Live imaging of *TgBAC(gng8:nfsB-EGFP-CAAX)* larvae with the Hb-IPN pathway (A) intact or before and after (B) bilateral, (C) left or (D) right severing (white arrowheads) of the fasciculus retroflexus (FR) at 3 d. FR lesions were confirmed at 8 d following behavioral testing. The left (L) and right (R) dHb are indicated. Scale bar is 50 m. (A′–D′). Corresponding locomotor activity measured in 1 sec intervals pre- and post-shock. Mean activity (solid black line) relative to pre-shock levels (dashed line), and standard error (light gray) are indicated. The y-axis is split (dotted line) to include heightened activity during

shock (gold box). (E) Locomotor activity was decreased in larvae with the left FR severed (n=20; Kruskal-Wallis ANOVA H=54.35, $p<0.0001$; Dunn's post-test; $p<0.05$) relative to uncut controls (n=9) or those with the right FR severed (n=19), and (F) duration of freezing also increased (n=20; Kruskal-Wallis ANOVA H=35.75, $p<0.01$; Dunn's post test, $p<0.05$). Horizontal bars representing mean ±SEM for 1-min intervals pre- and post-shock are superimposed over scatter plots of individual larvae (circles). No significance (ns) and significance below p=0.05 (*) are denoted. See also Figure S1 and S2.

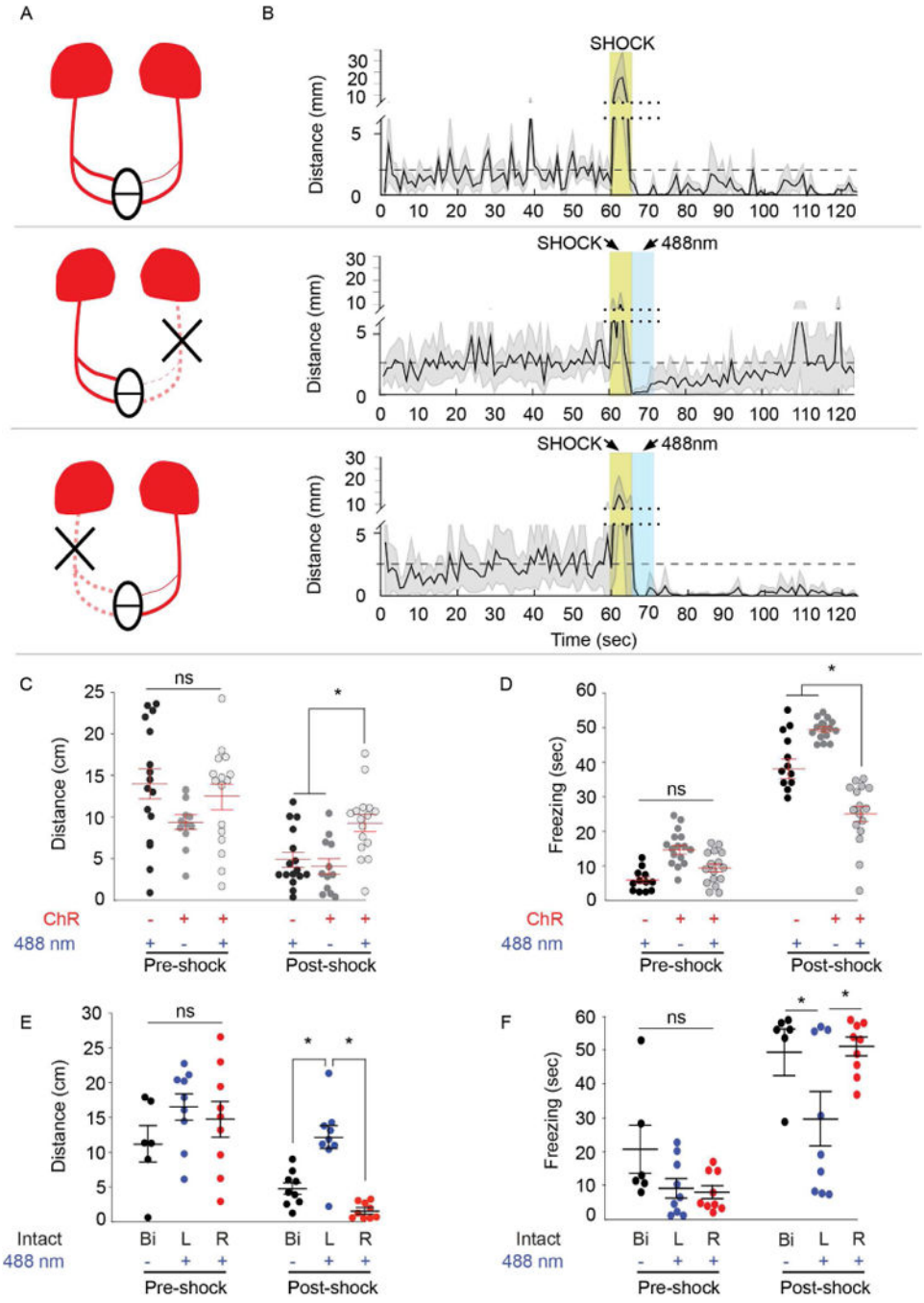

Fig. 2. Optogenetic activation of left dHb reduces freezing

(A) Schematic of dHb-IPN pathway with ChR2-mCherry transgene labeling in red. Optogenetic activation of only the left (middle) or right (bottom) dHb is achieved by severing (X) the contralateral FR. (B) Corresponding locomotor activity measured in 1 sec intervals during and post-shock, relative to pre-shock levels (dashed line). Mean (solid black line) and standard error (light gray) are indicated for larvae expressing ChR2 in the absence of blue light, or larvae with unilateral FR exposed to blue light. Not shown is a fourth group lacking ChR2 also tested for their response to blue light (refer to C). The y-axis is split

(dotted line) to include heightened activity during shock (gold box), which in some experiments is immediately followed by blue light (488 nm, blue box). (C) Compared to control larvae lacking mCherry labeling (black; n=16) or those not exposed to blue light (dark gray; n=12), optogenetic activation of both dHb (light gray; n=16) increased swimming post-shock (Kruskal-Wallis ANOVA $H=34.13$, $p<0.0001$; Dunn's post-test, $p<0.05$). (D) Bilateral activation of the dHb also significantly reduced freezing duration (Kruskal-Wallis ANOVA $H=73.23$; $p<0.0001$; Dunn's post test, $p<0.001$). (E) Optogenetic activation of just the left dHb (L, blue; n=9) post-shock increased locomotor activity (Kruskal-Wallis ANOVA $H=29.37$; $p<0.001$; Dunn's post test, $p<0.05$) and (F) reduced freezing (Kruskal-Wallis ANOVA $H=29.11$; $p<0001$, Dunn's post test, $p<0.05$) compared to larvae with the right side activated (R, red; n=9) or controls with intact bilateral FR not exposed to blue light (Bi, black; n=6). Horizontal bars representing mean ±SEM for 1-min intervals pre- and post-shock are superimposed over scatter plots of individual larvae (circles). No significance (ns) and significance below $p=0.05$ (*) are denoted. See also Figures S1 and S3.

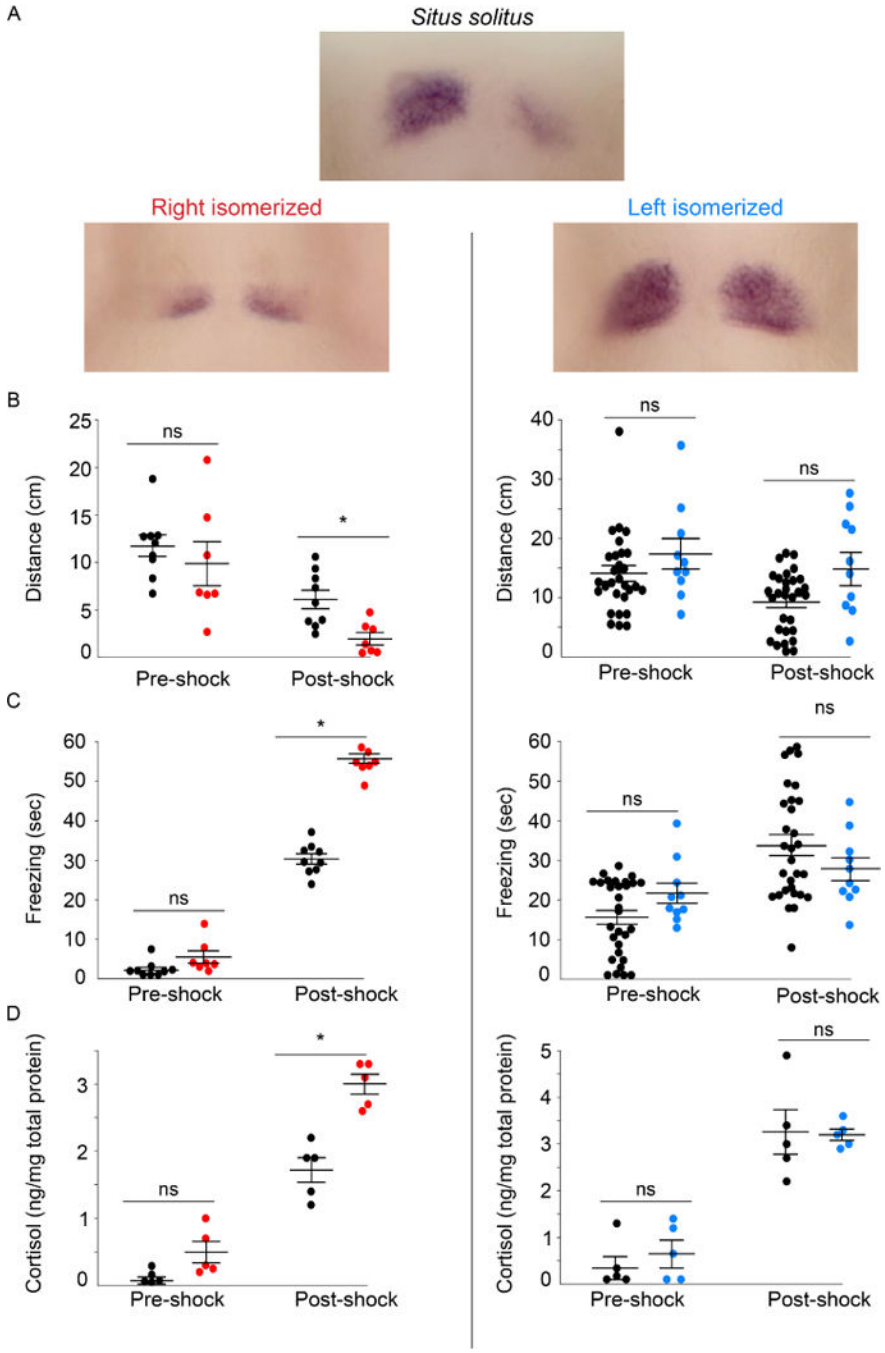

Fig. 3. Fear responses are diminished by dHb with left identity

(A) Expression pattern of *kctd12.1* in 7–8 d larvae with typical situs (*situs solitus*) and those with right (red) or left (blue) isomerized dHb. Following shock, larvae with right isomerized dHb (n=7) show (B) a significant reduction in swimming (Mann-Whitney U=6; p<0.01), and a significant increase in (C) freezing duration (Mann-Whitney U=91; p<0.001) and (D) cortisol levels (Mann-Whitney U=0; p<0.001) compared to controls (n=9). Significant differences were not observed between larvae with left isomerized dHb (n=10) and their wild-type siblings (n=30) for (B′) distance traveled (Mann-Whitney U=110; p = 0.221), (C′)

freezing duration (Mann-Whitney U=71; p=0.07) or (D′) cortisol levels (averaged from 5 pools of 15 larvae; Mann-Whitney U=10.5; p=0.7302) post-shock. Horizontal bars representing mean ±SEM are superimposed over scatter plots of individual larvae (circles). In B and C, pre- and post-shock measurements correspond to 1-min intervals. No significance (ns) and significance below p=0.05 (*) are denoted. See also Figure S1.

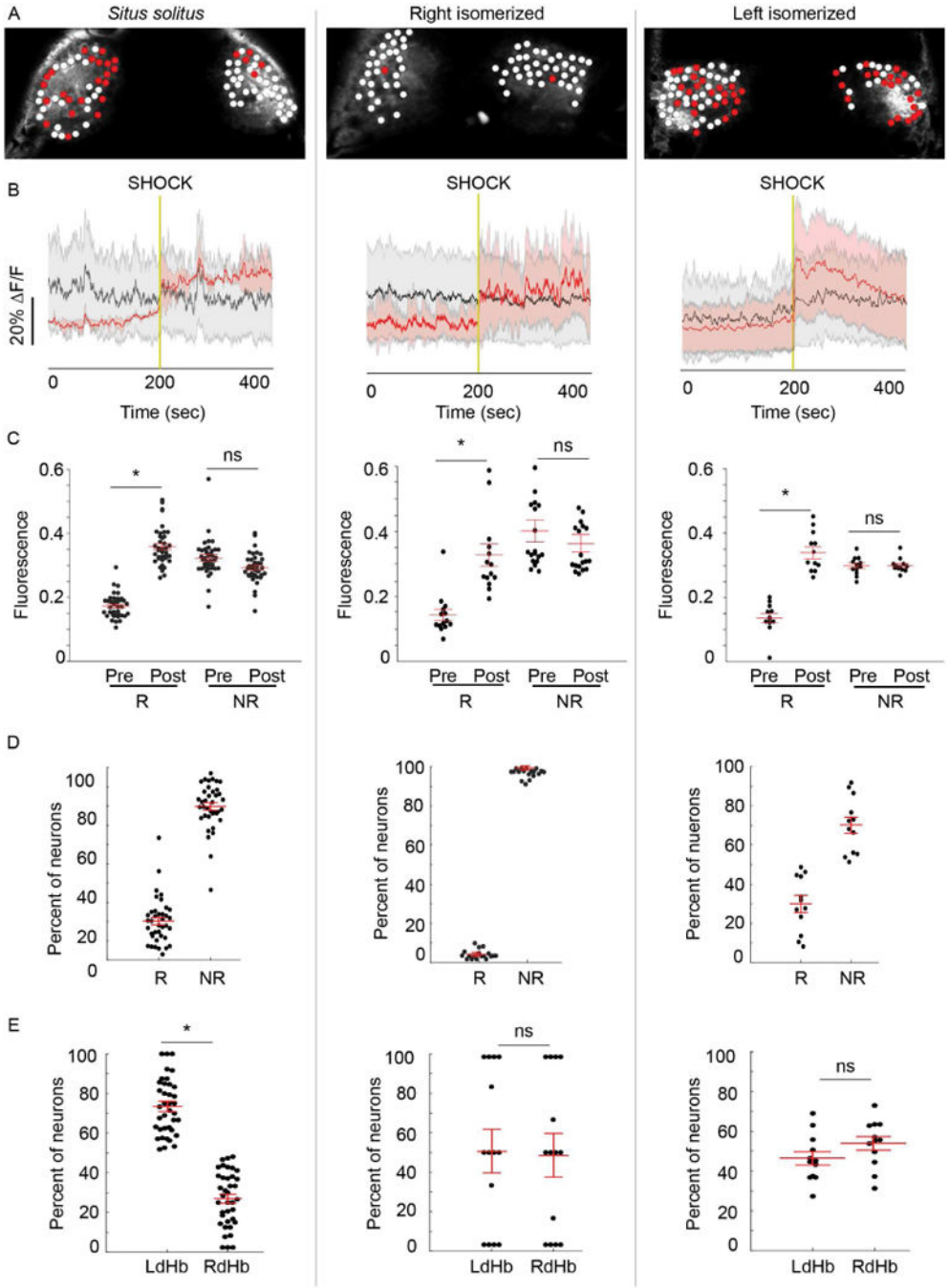

Fig. 4. Activation of neurons with left dHb identity is correlated with behavioral recovery

(A) Confocal images of dHb in 7–8 d *Tg(gng8:gal4ff)*; *Tg(UAS:GCaMP7a)* larvae. Red circles mark neurons that show increased activation post-shock and white circles those that are unchanged. (B) Average change in fluorescence intensity (ΔF/F) for responsive (red) and unresponsive (gray) neurons. Red and black lines represent the mean for all dHb neurons tested (n=4195 in 38 *situs solitus* from 8 clutches; n=1246 in 18 right isomerized from 4 clutches; n=1068 in 12 left isomerized from 4 clutches), and the shaded areas represent standard error of the mean. Vertical gold line indicates time of shock. (C) Mean fluorescence

intensity, calculated as the area under the curve, during 200 sec pre- (Pre) and post-shock (Post) intervals for responsive (R) and nonresponsive (NR) neurons. Mean fluorescence was significantly elevated post-shock in all configurations (*situs solitus*, Wilcoxon W=741, p<0.0001; right isomerized, Wilcoxon W=105, p<0.0001; left isomerized, Wilcoxon W=105, p<0.0001). However, (D) far fewer neurons were responsive in right isomerized dHb (Kruskal-Wallis ANOVA H=50.4, *situs solitus*, 20.2% ±2.0; right isomerized, 2.4% ±0.6, Dunn's post test p<0.0001; left isomerized, 30.0% ±4.1, Dunn's post test p<0.0001). (E) Responsive neurons are more abundant in the left dHb of *situs solitus* larvae (left; Wilcoxon W=741, p<0.0001), but are distributed equally between both dHb in right (Wilcoxon W=1, p>0.05) and left isomerized individuals (Wilcoxon W=81, p>0.05). Black circles in C–E correspond to individual larvae, and red bars represent mean ±SEM superimposed over each scatter plot. No significance (ns) and significance below p=0.05 (*) are denoted. See also Figures S3, S4 and Movie S2.